CHIN. PHYS. LETT. Vol. 32, No. 12 (2015) 121203

Discussion of Various Susceptibilities within Thermal and Dense Quantum Chromodynamics *

XU Shu-Sheng(徐书生)[1,5], SHI Yuan-Mei(石远美)[1,2], YANG You-Chang(杨友昌)[1,3], CUI Zhu-Fang(崔著钫)[1,5], ZONG Hong-Shi(宗红石)[1,4,5]**

[1]*Department of Physics, Nanjing University, Nanjing 210093*
[2]*Department of Physics and Electronic Engineering, Nanjing Xiaozhuang University, Nanjing 211171*
[3]*School of Physics and Mechanical-Electrical Engineering, Zunyi Normal College, Zunyi 563002*
[4]*Joint Center for Particle, Nuclear Physics and Cosmology, Nanjing 210093*
[5]*State Key Laboratory of Theoretical Physics, Institute of Theoretical Physics, Chinese Academy of Sciences, Beijing 100190*

(Received 15 August 2015)

It is commonly accepted that the system undergoes a crossover at high temperature and low chemical potential beyond the chiral limit case, and the properties of the crossover region are important for researchers to understand the nature of strong interacting matters of quantum chromodynamics (QCD). Since at present there is no exact order of parameters of the phase transitions beyond the chiral limit, QCD susceptibilities are widely used as indicators. In this work various susceptibilities are discussed in the framework of Dyson–Schwinger equations. The results show that different kinds of susceptibilities give the same critical end point, which is the bifurcation point of the crossover region and the first order phase transition line of QCD. Nevertheless, different pseudo-critical points are found in the temperature axis. We think that defining a critical band is more suitable in the crossover region.

PACS: 12.39.−x, 12.39.Fe, 25.75.Nq DOI: 10.1088/0256-307X/32/12/121203

Dynamical chiral symmetry breaking (DCSB) and confinement are two important features of quantum chromodynamics (QCD). Chiral symmetry and its spontaneous breaking at low temperatures also play important roles in understanding the phase diagram of QCD. The phase structure of QCD at finite temperature T and chemical potential μ have attracted great efforts in both theory and experiments. It is generally believed that there is a Nambu phase (chiral symmetry breaking phase) in the region of low T and μ, and a Wigner phase (chiral symmetry restored phase) in the region of high T and/or μ. In recent years, there has been valuable progress in both lattice QCD (LQCD) and effective models of QCD.

One of the most important findings is the strong correlation in the quark–gluon plasma (QGP) with temperature above the critical temperature.[1] It implies that QCD is still non-perturbative in high temperature. Even though LQCD is a powerful approach to study non-perturbative phenomena, there is intrinsic difficulty in dealing with the case of finite chemical potential μ because of its sign problem. Hence, some effective models are used to study thermal and dense QCD inevitably, such as the Nambu–Jona–Lasinio (NJL) model,[2–8] the QCD sum rules,[9–12] lattice QCD,[13–17] and the Dyson–Schwinger equations (DSEs).[18–27]

In the chiral limit case (the current quark mass $m = 0$), it is expected that the chiral symmetry is restored from low to high T and μ. The two-quark condensate would change to zero at certain points of T and μ, thus it can be regarded as an order parameter of the chiral phase transition. In the region of low T, the first-order phase transition happens at some certain μ. It is apparent that there is a tri-critical point (TCP) in the phase diagram, while beyond the chiral limit, there is still no rigorous order parameter from first principles of QCD. In quantum field theory, various QCD susceptibilities are the linear responses of QCD condensate to various variables (such as the temperature, the current mass and the chemical potential). Various susceptibilities are often used to fix the critical point of chiral phase transition,[26,32–37] which is similar to the case of chiral limit.

In the Euclidean space, the gap equation at finite T and μ reads

$$S^{-1}(\boldsymbol{p},\tilde{\omega}_n) = S_0^{-1}(\boldsymbol{p},\tilde{\omega}_n) + \frac{4}{3}T\sum_{l=-\infty}^{\infty}\int\frac{d^3q}{(2\pi)^3} \times g^2 D_{\mu\nu}(\boldsymbol{p}-\boldsymbol{q},\tilde{\omega}_n-\tilde{\omega}_l)\gamma_\mu \cdot S(\boldsymbol{q},\tilde{\omega}_l)\Gamma_\nu(\boldsymbol{q},\tilde{\omega}_l,\boldsymbol{p},\tilde{\omega}_n), \quad (1)$$

where $S_0(\boldsymbol{p},\tilde{\omega}_n)$ is the bare quark propagator, $\tilde{\omega}_n = \omega_n + i\mu$ with $\omega_n = (2n+1)\pi T$, $n \in Z$ the fermion

*Supported by the National Natural Science Foundation of China under Grant Nos 11275097, 11475085, 11535005, and 11265017, the Jiangsu Planned Projects for Postdoctoral Research Funds under Grant No 1402006C, the China Postdoctoral Science Foundation under Grant No 2015M571728, the Natural Science Foundation of Jiangsu Province under Grant No BK20130078, and the Guizhou-Provincial Outstanding Youth Science and Technology Talent Cultivation Object Special Funds under Grant No QKHRZ(2013)28.

**Corresponding author. Email: zonghs@nju.edu.cn

© 2015 Chinese Physical Society and IOP Publishing Ltd

Matsubara frequencies, $D_{\mu\nu}$ is the dressed gluon propagator, and $\Gamma_\nu(\boldsymbol{q},\tilde{\omega}_l,\boldsymbol{p},\tilde{\omega}_n)$ is the dressed quark–gluon vertex.

The rainbow truncation is widely used in studying hadron physics and thermal QCD, that is,

$$\Gamma_\nu(\boldsymbol{q},\tilde{\omega}_l,\boldsymbol{p},\tilde{\omega}_n)=\gamma_\nu. \tag{2}$$

The model of dressed gluon propagator adopted in this work is[38]

$$g^2D_{\mu\nu}(\boldsymbol{p}-\boldsymbol{q},\tilde{\omega}_n-\tilde{\omega}_l)=D\frac{4\pi^2}{\omega^6}\kappa e^{-\kappa/\sigma^2}P^T_{\mu\nu}, \tag{3}$$

where $\kappa=(\boldsymbol{p}-\boldsymbol{q})^2+(\omega_n-\omega_l)^2$, and $P^T_{\mu\nu}$ is the transverse projection operator. It is worth noting that this model is a simplified model in Ref. [39], in which the properties of pseudo-scalar and vector meson can be described well. To make our study quantitatively reliable, it is important to constrain model parameters with already known precise information from lattice QCD at zero density. The parameters in Eq. (3), D and ω, and light quark mass m are fixed by fitting the temperature dependence of the quark condensate from lattice QCD,[40] as displayed in Fig. 1, where $D=1.2$, $\omega=0.5$ and the light quark mass $m=10\,\mathrm{MeV}$ are used.

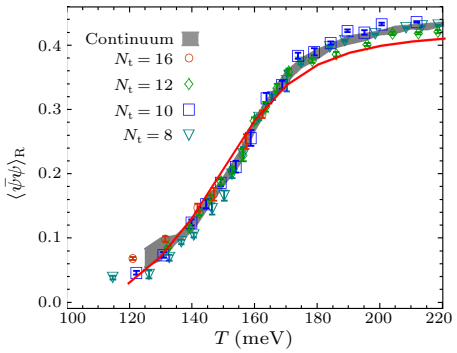


Fig. 1. (Color online) The results of lattice QCD in Ref. [40] and the fitting (solid and red lines) in our model study.

Within those approximations, the solution of the quark propagator can be generally written, via the Lorentz structure analysis, as follows:

$$\begin{aligned}S^{-1}(\boldsymbol{p},\tilde{\omega}_n)=&i\boldsymbol{\gamma}\cdot\boldsymbol{p}A(\boldsymbol{p}^2,\tilde{\omega}_n^2)+i\gamma_4\tilde{\omega}_nC(\boldsymbol{p}^2,\tilde{\omega}_n^2)\\&+B(\boldsymbol{p}^2,\tilde{\omega}_n^2)+\gamma_4\boldsymbol{\gamma}\cdot\boldsymbol{p}D(\boldsymbol{p}^2,\tilde{\omega}_n^2),\end{aligned} \tag{4}$$

with, e.g., $B(\boldsymbol{p},\omega_n)^*=B(\boldsymbol{p},\omega_{-n-1})$, where the scalar functions A, B, C, D can be solved numerically by the direct iteration. However, $D(\boldsymbol{p}^2,\tilde{\omega}_n^2)$ is almost vanished in our study.

Formally, the two-quark condensate can be expressed by means of dressed quark propagator,

$$\langle\bar{\psi}\psi\rangle=-N_cN_fT\sum_{n=-\infty}^{\infty}\int\frac{d^3q}{(2\pi)^3}\mathrm{Tr}[S(\boldsymbol{p},\tilde{\omega}_n)], \tag{5}$$

where the notation Tr denotes trace over Dirac indexes, and the dressed quark propagator is

$$\begin{aligned}S(\boldsymbol{p},\tilde{\omega}_n)=&-i\boldsymbol{\gamma}\cdot\boldsymbol{p}\sigma_A(\boldsymbol{p},\tilde{\omega}_n)-i\gamma_4\tilde{\omega}_n\sigma_C(\boldsymbol{p},\tilde{\omega}_n)\\&+\sigma_B(\boldsymbol{p},\tilde{\omega}_n),\end{aligned} \tag{6}$$

with

$$\begin{aligned}&\sigma_F(\boldsymbol{p},\tilde{\omega}_n)\\=&\frac{F(\boldsymbol{p},\tilde{\omega}_n)}{\boldsymbol{p}^2A^2(\boldsymbol{p},\tilde{\omega}_n)+\tilde{\omega}_n^2C^2(\boldsymbol{p},\tilde{\omega}_n)+B^2(\boldsymbol{p},\tilde{\omega}_n)},\end{aligned} \tag{7}$$

where F can be A, B and C. It is worth noting that there is a linear divergence in the formula of two-quark condensate beyond the chiral limit, that is, Eq. (5). To obtain some meaningful results, the two-quark condensate of bare quark propagator is subtracted. The regularized two-quark condensate is defined as

$$\begin{aligned}\langle\bar{\psi}\psi\rangle=&-N_cN_fT\sum_{n=-\infty}^{\infty}\int\frac{d^3q}{(2\pi)^3}\mathrm{Tr}[S(\boldsymbol{p},\tilde{\omega}_n)\\&-S_0(\boldsymbol{p},\tilde{\omega}_n)],\end{aligned} \tag{8}$$

with

$$S_0(\boldsymbol{p},\tilde{\omega}_n)=\frac{-i\boldsymbol{\gamma}\cdot\boldsymbol{p}-i\gamma_4\tilde{\omega}_n+m}{\boldsymbol{p}^2+\tilde{\omega}_n^2+m^2}. \tag{9}$$

The two-quark condensate can be calculated directly via Eq. (8), if only the dressed quark propagator is solved by gap equation in the T–μ plane. The varying of $\langle\bar{\psi}\psi\rangle$ with μ at different T is shown in Fig. 2. There is a discontinuity of $\langle\bar{\psi}\psi\rangle$ at a certain chemical potential $\mu=\mu_0(T)$ for each temperature $T<80\,\mathrm{MeV}$. It implies that a first order phase transition appears at $\mu=\mu_0(T)$ with an arbitrary $T<80\,\mathrm{MeV}$. The chiral symmetry broken phase turns to the symmetry preserved phase with the increase of μ. We can also see from Fig. 2 that $\langle\bar{\psi}\psi\rangle$ is continuum when $T>80\,\mathrm{MeV}$, while the susceptibility $\frac{\partial\langle\bar{\psi}\psi\rangle}{\partial\mu}$ tends to infinity at some certain $\mu=\mu_0(T)$ when $T>80\,\mathrm{MeV}$. This means that a second order phase transition occurs with increasing μ in the region of $T>80\,\mathrm{MeV}$.

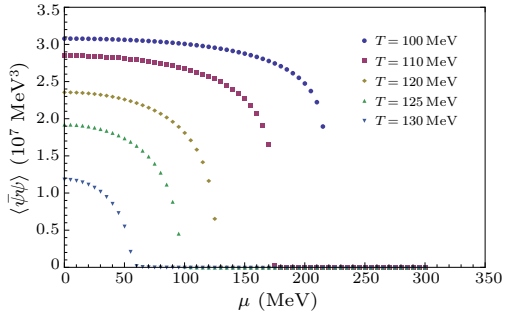


Fig. 2. (Color online) Dependence of the two-quark condensate $\langle\bar{\psi}\psi\rangle$ on temperature T and chemical potential μ in the chiral limit.

For small current quark mass, the chiral symmetry is broken slightly in the original Lagrangian, i.e., the axial-vector current is partially conserved. In this

study, we fix the current quark mass m=10 MeV. Rigorously speaking, there is no chiral symmetry restored phase in this case. However, we can see from Fig. 3 that there is a discontinuity of the two-quark condensate at some certain μ when $T < 128$ MeV. This indicates that there are two different phases, i.e., the so-called chiral symmetry breaking phase and the chiral symmetry partial restoration phase. In the region $T < 128$ MeV, the QCD system suffers a chiral phase transition with the increase of μ.

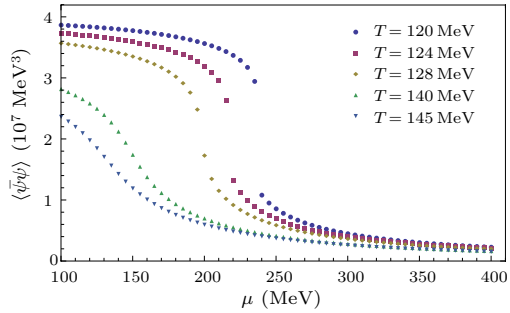


Fig. 3. (Color online) Dependence of the two-quark condensate $\langle\bar{\psi}\psi\rangle$ on temperature T and chemical potential μ beyond the chiral limit.

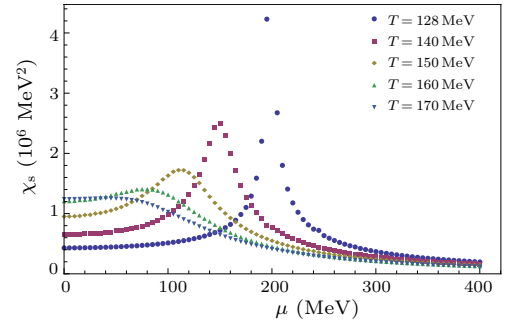


Fig. 4. (Color online) Dependence of the chiral susceptibility χ_s on temperature T and chemical potential μ beyond the chiral limit.

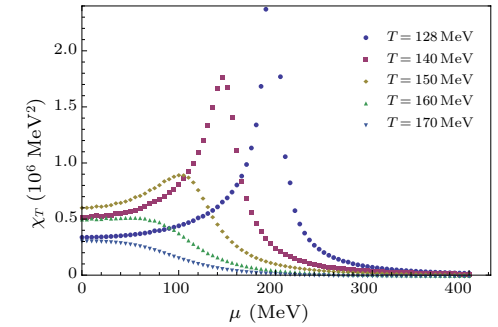


Fig. 5. (Color online) Dependence of the temperature susceptibility χ_T on temperature T and chemical potential μ beyond the chiral limit.

For such a phase transition, the two-quark condensate is also viewed as the order parameter, even though it is not rigorous anymore. The critical end point (CEP) is located at $(T_E, \mu_E) = (128,200)$ MeV. For $T > T_E$, the condensate is continuous, and the peak of the susceptibility $\frac{\partial\langle\bar{\psi}\psi\rangle}{\partial\mu}$ becomes finite. This implies that the area becomes crossover contrast with the second order transition in the chiral limit case.

Researchers always define an artificially critical point, also called the pseudo-critical point, to describe the rapid change of thermodynamical properties in the crossover region. It is certain that the criteria for the critical point are the extremum of susceptibilities, such as chiral susceptibility and temperature susceptibility.

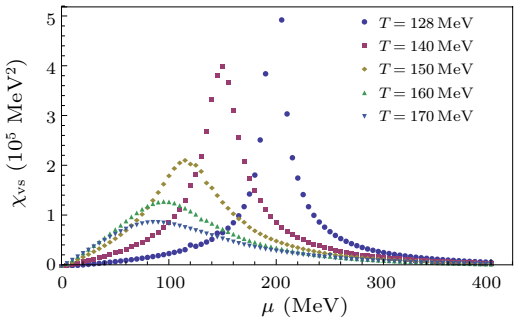


Fig. 6. (Color online) Dependence of the vector–scalar susceptibility χ_{vs} on temperature T and chemical potential μ beyond the chiral limit.

Let us introduce three kinds of susceptibilities: (i) the chiral susceptibility χ_s, (ii) the temperature susceptibility χ_T, and (iii) the vector–scalar susceptibility χ_{vs}. Combined with Eq. (8), their definitions and expressions are as follows:

$$\chi_s \equiv -\frac{\partial\langle\bar{\psi}\psi\rangle}{\partial m}, \tag{10}$$

$$\chi_T \equiv -\frac{\partial\langle\bar{\psi}\psi\rangle}{\partial T}, \tag{11}$$

$$\chi_{vs} \equiv -\frac{\partial\langle\bar{\psi}\psi\rangle}{\partial \mu}. \tag{12}$$

Together with Eq. (4) solved by a gap equation, three susceptibilities, i.e., Eqs. (10)–(12), can be calculated directly. The chiral susceptibility, temperature susceptibility and vector–scalar susceptibility varying with the chemical potential at different temperatures in the crossover region are shown in Figs. 4–6, respectively. We can see from Fig. 4 that the peak of the chiral susceptibility is decreasing as the temperature increases. Our numerical results show that the pseudo-critical point is located at $T = 170$ MeV when $\mu = 0$. It is depicted in Fig. 5 that the behavior of temperature susceptibility is very similar to the chiral susceptibility, while the pseudo-critical point is located at $T = 160$ MeV (as a comparison, LQCD gives $T = 155^{\pm 3}$ MeV[40]). The behavior of vector–scalar susceptibility in Fig. 6 is slightly different from the other two susceptibilities, especially at $\mu = 0$. We can see from Fig. 6 that the vector–scalar susceptibility is 0 at $\mu = 0$ with arbitrary temperature, which can be illustrated by means of another auxiliary susceptibility

$$\chi_m \equiv -\frac{\partial\langle\psi^\dagger\psi\rangle}{\partial m}. \tag{13}$$

There is a relation between vector-scalar suscepti-

bility and the auxiliary susceptibility,[41]

$$\chi_m = -\frac{\partial\langle\psi^\dagger\psi\rangle}{\partial m} = \frac{T}{V}\frac{\partial^2 \ln \mathcal{Z}}{\partial m \partial\mu} = -\frac{\partial\langle\bar{\psi}\psi\rangle}{\partial\mu} = \chi_{\rm vs}, \quad (14)$$

where $\mathcal{Z}$ is the QCD partition function, and the quark number density is expressed as

$$\begin{aligned}\langle\psi^\dagger\psi\rangle &= -N_{\rm c}N_{\rm f}\,T\sum_{n=-\infty}^{\infty}\int\frac{d^3q}{(2\pi)^3}{\rm Tr}[S(\boldsymbol{p},\tilde{\omega}_n)\gamma_4] \\ &= 4iN_{\rm c}N_{\rm f}T\sum_{-\infty}^{+\infty}\int\frac{d^3\boldsymbol{q}}{(2\pi)^3}\frac{\tilde{\omega}_n C(\boldsymbol{q},\tilde{\omega}_n)}{\boldsymbol{q}^2A^2+q_4^2C^2+B^2}, \quad (15)\end{aligned}$$

where A, B and C all are functions of $(\boldsymbol{p},\tilde{\omega}_n)$. If $\mu = 0$, A, B and C will be real and even functions of arguments $(\boldsymbol{q},\tilde{\omega}_n)$, that is,

$$F(\boldsymbol{p},\tilde{\omega}_n) = F(\boldsymbol{p},\tilde{\omega}_{-n-1}) = F(-\boldsymbol{p},\tilde{\omega}_n), \quad (16)$$

where F denotes A, B and C, then, the integrand in Eq. (15) is an odd function of ω_n and an even function of $\boldsymbol{p}$, and one can conclude

$$\langle\psi^\dagger\psi\rangle|_{\mu=0} = 0 \quad (17)$$

at arbitrary temperature and current quark mass, hence

$$\chi_{\rm vs}|_{\mu=0} = \chi_m|_{\mu=0} = 0 \quad (18)$$

for arbitrary T.

According to different criteria for the pseudo-critical point, we can see from Figs. 4–6 that these three susceptibilities give the same location of CEP. However, they give different pseudo-critical points in the crossover region. There is no pseudo-critical point at $\mu = 0$ for $\chi_{\rm vs}$ due to the fact that $\chi_{\rm vs} = 0$ at $\mu = 0$ with arbitrary temperature. These results imply that there is a critical band in the crossover region, which deserves further discussion.

In summary, we have studied the chiral phase transition in the chiral limit and beyond the framework of DSEs, the parameters are fitted by LQCD's results. A second-order phase transition occurs at high temperatures and in the low chemical potential region in the chiral limit case, while the region becomes crossover beyond the chiral limit case, and the first-order phase transition is still held. We find that three kinds of susceptibilities locate at the same CEP, but in the crossover region, especially at low chemical potential, these susceptibilities give different results. The chiral susceptibility and the temperature susceptibility give similar results, while vector–scalar susceptibility is vanished at low chemical potential. We conclude that it is more suitable to define a critical band in the crossover region. We will improve the gluon model (for example, including temperature effects) and study this further.

References

[1] Asakawa M and Hatsuda T 2004 *Phys. Rev. Lett.* **92** 012001
[2] Vogl U and Weise W 1991 *Prog. Part. Nucl. Phys.* **27** 195
[3] Klevansky S P 1992 *Rev. Mod. Phys.* **64** 649
[4] Hatsuda T and Kunihiro T 1994 *Phys. Rep.* **247** 221
[5] Buballa M 2005 *Phys. Rep.* **407** 205
[6] Cui Z F et al 2013 *Eur. Phys. J.* C **73** 2612
Cui Z F, Shi C, Sun W M, Wang Y L and Zong H S 2014 *Eur. Phys. J.* C **74** 2782
[7] Shi S, Yang Y C, Xia Y H, Cui Z F, Liu X J and Zong H S 2015 *Phys. Rev.* D **91** 036006
[8] Kohyama H, Kimura D and Inagaki T 2015 *Nucl. Phys.* B **896** 682
[9] Reinders L J, Rubinstein H and Yazaki S 1985 *Phys. Rep.* **127** 1
[10] King I and Sachrajda C T 1987 *Nucl. Phys.* B **279** 785
[11] Hatsuda T and Lee S H 1992 *Phys. Rev.* C **46** R34
[12] Klingl F, Kaiser N and Weise W 1997 *Nucl. Phys.* A **624** 527
[13] Borsanyi S et al 2010 *J. High Energy Phys.* **1009** 073
[14] Ejiri S and Yamada N 2013 *Phys. Rev. Lett.* **110** 172001
[15] Forcrand P D, Langelage J, Philipsen O and Unger W 2014 *Phys. Rev. Lett.* **113** 152002
[16] Braguta V V, Goy V A, Ilgenfritz E M, Kotov A Y, Molochkov A V, Muller-Preussker M and Petersson B 2015 *J. High Energy Phys.* **1506** 094
[17] Endrodi G 2015 *J. High Energy Phys.* **1507** 173
[18] Roberts C D and Williams A G 1994 *Prog. Part. Nucl. Phys.* **33** 477
Roberts C D and Schmidt S M 2000 *Prog. Part. Nucl. Phys.* **45** S1
[19] Alkofer R and Smekal L V 2001 *Phys. Rep.* **353** 281
[20] Jiang Y, Chen H, Sun W M and Zong H S 2013 *J. High Energy Phys.* 1304 14
Shi C, Wang Y L, Jiang Y, Cui Z F and Zong H S 2014 *J. High Energy Phys.* 1407 14
[21] Cloet I C and Roberts C D 2014 *Prog. Part. Nucl. Phys.* **77** 1
[22] Gutierrez E, Ahmad A, Ayala A, Bashir A and Raya A 2014 *J. Phys.* G **41** 075002
[23] Zhao A M, Cui Z F, Jiang Y and Zong H S 2014 *Phys. Rev.* D **90** 114031
[24] Wang B, Wang Y L, Cui Z F and Zong H S 2015 *Phys. Rev.* D **91** 034017
Xu S S, Cui Z F, Wang B, Shi Y M, Yang Y C and Zong H S 2015 *Phys. Rev.* D **91** 056003
[25] Zhu H X, Sun W M and Zong H S 2013 *Chin. Phys. Lett.* **30** 051201
[26] Tian Y L, Cui Z F, Wang B, Shi Y M, Yang Y C and Zong H S 2015 *Chin. Phys. Lett.* **32** 081101
[27] Jiang Y, Hou F Y, Luo C B and Zong H S 2015 *Chin. Phys. Lett.* **32** 021201
[28] Zong H S, Hou F Y, Sun W M, Ping J L and Zhao E G 2005 *Phys. Rev.* C **72** 035202
[29] Zong H S, Shi Y M, Sun W M and Ping J L 2006 *Phys. Rev.* C **73** 035206
[30] Shi Y M, Wu K P, Sun W M, Zong H S and Ping J L 2006 *Phys. Lett.* B **639** 248
[31] Chang L, Liu Y X, Sun W M and Zong H S 2008 *Phys. Lett.* B **669** 327
[32] Chang L, Liu Y X, Roberts C D, Shi Y M, Sun W M and Zong H S 2009 *Phys. Rev.* C **79** 035209
[33] Cui Z F, Hou F Y, Shi Y M, Wang Y L and Zong H S 2015 *Ann. Phys. (N. Y.)* **358** 172
[34] Qin S X, Chang L, Chen H, Liu Y X and Roberts C D 2011 *Phys. Rev. Lett.* **106** 172301
[35] Maris P and Roberts C D 1997 *Phys. Rev.* C **56** 3369
[36] Borsanyi S, Fodor Z, Hoelbling C, Katz S D, Krieg S, Ratti C and Szabo K K 2010 *J. High Energy Phys.* **1009** 73
[37] Du Y L, Cui Z F, Xia Y H and Zong H S 2013 *Phys. Rev.* D **88** 114019